ngr-33-008-012 Mr. Quinn Code Y

X-RAY STRUCTURE OF THE CYGNUS LOOP*

P. Gorenstein, B. Harris, H. Gursky, R. Giacconi
American Science and Engineering, Inc.
Cambridge, Massachusetts 02142

and

R. Novick and P. Vanden Bout
Columbia Astrophysics Laboratory
Columbia University, New York, New York 10027

Submitted to Science
December 1970

*Columbia Astrophysics Laboratory Contribution No. 36.

X-RAY STRUCTURE OF THE CYGNUS LOOP

P. Gorenstein, B. Harris, H. Gursky, R. Giacconi
American Science and Engineering, Inc.
Cambridge, Massachusetts 02142

and

R. Novick and P. Vanden Bout
Columbia Astrophysics Laboratory
Columbia University, New York, New York 10027

ABSTRACT

X-ray emission from the Cygnus Loop was observed in the energy region .2 - 1keV with a collector that focused x-rays along one dimension while scanning across the nebula. The total integrated intensity is 1.3 x 10^{-8} ergs/cm^2-sec. The one dimensional x-ray structure has the same angular size $\sim 3^{\circ}$ as the outermost boundaries of the optical filaments. There is no increase in x-ray emission at the center of the nebula nor at the strong feature that is seen in certain radio maps. The x-ray spectrum is consistent with thermal radiation from a hot plasma at a temperature of about 4 x 10^{6} °K with evidence for a line at 19Å corresponding to the 2P→1S transition of OVIII.

X-ray emission from the supernova remnant known as the Cygnus Loop or Veil Nebula was observed in the energy range .2 - 1keV from an attitude controlled Aerobee 170 sounding rocket that was launched 4:55UT on 26 June 1970 from the White Sands Missile Range. A recent article by Grader, Hill and Stoering(1) has reported intense x-ray emission in this range from an extended object which they identified with the Cygnus Loop. Also this object is very likely coincident with the x-ray source Vul XR-1 which had been reported previously with an imprecise location(2).

The purposes of this observation were to: 1. obtain a precise location that would confirm the identification by Grader et al of the extended x-ray source with the Cygnus Loop; 2. obtain a high resolution mapping of the x-ray emission that could be correlated with the optical and radio pictures of the Cygnus Loop; 3. distinguish between a thermal and non-thermal mechanism on the basis of a spectral analysis of the x-ray data.

A rather unique instrumentation system based on focusing x-ray optics by means of grazing incidence reflection was used in this observation. For x-ray wavelengths exceeding 10Å, the potential advantages of focusing compared to conventional systems are better angular resolution and an improved ratio of signal-to-noise by virtue of the fact that the focused image is considerably smaller than the collecting area. Hence, the detector can be small and less influenced by cosmic ray effects. Also the reflecting surfaces effectively block the direct path of soft charged particles that are sporadically present in the space environment. These particles would otherwise penetrate the thin entrance window of the detector and add to the background level. This particular instrument consists of a collector that focuses radiation in one dimension upon a multi-element x-ray detector in the focal plane. The collector consists of eight nested reflecting plates whose dimensions are 20cm x 40cm and is symmetric about the central plane. Each plate is curved slightly to approximate a parabola in one dimension and focuses to a common line. The overall field of view of the instrument is

2° along the direction of focusing and 9° along the perpendicular direction.

The eight reflecting surfaces are commercial 1mm thick float glass overcoated with an evaporated layer of 1500Å of chromium for improved x-ray reflectivity at short wavelengths and are reenforced by a steel backing. The focal plane detector is two - four wire proportional counters with an entrance window of 1.3 microns of polypropylene. The wires were spaced at a distance equivalent to an angular separation of 0.5° which determines the angular resolution of the system. A regulated supply system of pure propane gas compensated for losses through the thin polypropylene windows by maintaining the pressure at a constant level of 50cm. of Hg. The energy resolution of the detectors gave a full width at half maximum in the pulse amplitude distribution of 100% for photon energies (wavelengths) of .28keV (44Å) and about 40% at 1.25keV (10Å). The entire system is sensitive in the wavelength bands 80 - 44Å (.16 - .28keV) and 20 - 10Å (.6 - 1.2keV). Photography of the star field at intervals of one second provided the aspect data. More instrumentation details are described elsewhere(3).

This observation took place during the later phases of the rocket flight prior to reentering the earth's atmosphere. X-ray data from other regions of the sky will be reported separately. Approximately 1500 net counts were obtained during a single scan across the Cygnus Loop that took place at a rate of $1/4^{\circ}$/second. Figure 1 shows the angular response of four independent detectors to the Cygnus Loop plus, for purposes of comparison, the response to well collimated radiation in the laboratory. With the aspect information count data from the four detectors can be properly combined and represented in celestial coordinates. The result is a one dimensional x-ray map of the Cygnus Loop that is shown superimposed upon a photograph of the optical filaments in Figure 2.

Several conclusions follow from a comparison of these maps. One, the size and structure of the x-ray emission is consistent with that of the shell-like region bounding the optical filaments. The diameter of the x-ray region is about 2.8°, like that of the outermost boundaries of the filaments. There is no increase in x-ray emission at the center of the nebula. Two, to within the resolution of the instrument, $1/2^{\circ}$, the level of x-ray emission declines rather sharply at the outer boundaries of the optical filaments. Three, the strong central feature that appears in a radio contour map(4) does not coincide with a strong maximum in the x-ray emission.

A spectral analysis was made of the pulse amplitude distribution of the counts from the Cygnus Loop. The usual procedure was followed; an assumed function of energy containing undetermined parameters is multiplied by all the known efficiencies and is convolved with a resolution function that simulates the pulse amplitude distribution response of the proportional counter to mono-energetic photons at any energy(5). For each set of parameter values the degree of agreement between the computed and observed pulse amplitude spectra is decided quantitatively on the basis of a minimum chi-square test. Grazing incidence telescopes require a correction for an energy dependent x-ray reflection efficiency. A theoretical efficiency function was computed for this particular instrument from the reflection properties of chromium as measured by Ershov, Brytov, and Lukirskii(6). The theoretical telescope efficiency was confirmed at 1.25keV by laboratory measurements.

At the estimated distance to the Cygnus Loop, 770pc(7), the opacity of the galaxy becomes significant for x-ray energies, E, less than 0.3keV. In the analysis a set of x-ray attenuation coefficients for the interstellar medium as recently computed by Brown and Gould(8) for revised helium and neon abundances were used to calculate $Tr(E, N_H)$, the interstellar transmission. The value of N_H, the number of hydrogen atoms along the line of sight was left as an undetermined parameter. The large volume of the Cygnus Loop precludes any internal absorption.

Two classes of spectral functions multiplied by interstellar transmission were considered:

(a) $$dN/dE = A\, Tr(E, N_H)\, E^{-\alpha}$$

(b) $$dN/dE = A\, Tr(E, N_H) \left\{ Exp\,(-E/kT)/E + B\ \delta\,(E - .65keV) \right\}$$

The quantities α, T, N_H, B, and A are the undetermined parameters. The two expressions represent alternative physical processes resulting in x-ray emission.

Expression (a) represents the type of spectrum that could be produced by synchrotron radiation, for example, the Crab Nebula. Expression (b) is an approximation to the thermal emission spectrum that one expects from a hot plasma that contains a cosmic elemental abundance. The actual spectrum would consist of a continuum plus a number of lines and recombination edges. It has been suggested that a line at 0.65keV corresponding to the 2P→1S transition of OVIII would be a prominent feature of the thermal x-ray emission from the boundaries of a shock wave that has been produced as a result of a supernova explosion expanding into the interstellar medium(9). We represent this feature by a delta function in expression (b).

The results of the analysis show that expression (a) is inconsistent with our data for all possible values of the spectral index, α. However, one can probably not exclude more complex expressions that might arise from synchrotron radiation, for example, a power law spectrum that is characterized by a large change in the spectral index between 20 and 15Å.

Expression (b) did fit the data with an acceptable value of the chi-square with a finite value for the strength of the line at 0.65keV (the quantity "B"). Since (b) is only an approximation to the actual spectrum of radiation from a hot plasma the temperature found as a result of fitting this expression is not necessarily the same as the true temperature of the plasma. The observed and computed pulse height distributions are shown in Figure 3. The parameters associated with the best (minimum chi-square) fit are:

$$T = 4.3 \times 10^{6} K$$

$$N_H = 2.6 \times 10^{20} \text{ Hatoms/cm}^2$$

Total Integrated Intensity = 1.5×10^{-8} ergs/cm^2-sec $\quad$ $E > .2$keV.

The most outstanding result of the analysis is that about one-third of the energy flux from the Cygnus Loop for $E > .2$keV is contained in a line at 0.65keV. If true, it is rather firm evidence that the source of the x-ray emission is a hot plasma and for the existence of high temperatures in old supernova remnants. Hence, it is important to examine this result rather carefully. Inspection of the raw pulse height data from the Cygnus Loop shows that there are a large number of counts between .55 and .75keV. This results in the line at .65keV in the analysis. This feature is not questionable on the basis of its statistical significance. If spurious it originates in systematic errors. The most important possible systematic errors are: incorrect reflection efficiency of the collector, and an incorrect energy calibration of the proportional counters. Both these effects would be confined to the region around .65keV as the other parameters we determine for the Cygnus Loop spectrum are in agreement with reference (1). As for the first effect it is true that the x-ray reflection efficiency of the chromium collector is undergoing large changes in the vicinity of the chromium L -edges. However, actual experimental values of reflectivity including edge effects as measured by Ershov et al(6) were used in the calculation of the collector efficiency function. Additional measurements at several wavelengths on chromium plates similar to the ones used in the collector confirmed the applicability of the theoretical reflectivity to our chromium surfaces. To simulate the effect of a line the value we used for the collector efficiency would have to be low by about a factor of two at .65keV. We feel that this large an error is unlikely. The other possible systematic error is an incorrect energy calibration of the proportional counter pulse amplitude response. The calibration is based on an irradiation of the counters with characteristic x-rays of .185, .282, .68 and 1.25keV several days before flight. One of the calibration points is very close in energy to the oxygen line. There are several indications from the flight data that the energy calibration is correct. A large increase in counting efficiency occurs below 0.28keV due to the K-edge of carbon in the detector window. In general the pulse height distribution reflects this feature. Errors in energy calibration would also distort other data as well as the Cygnus Loop. In the case of other events seen in this experiment both background data and another source, Cyg X-1, there are not indications of anomalies at 0.65keV, the energy of the line.

If we exclude the possibility that the spectral function is undergoing rapid changes in the wavelength interval of the observation, then the most likely form of the x-ray emission is radiation from a high temperature plasma. Hence the process responsible for the x-rays from the Cygnus Loop appears to be quite distinct from that of the Crab Nebula. This is not surprising in view of the large difference in age and volume between the objects. One now might consider the possibility that the large x-ray flux is responsible for the excitation of the optical line emission observed from the filaments of the Cygnus Loop. However, in the hot plasma hypothesis one encounters the difficulty of explaining the lack of consistency between the high temperature observed in the x-ray region and the apparent low expansion velocity of the filaments.

We now know of two classes of x-ray sources among the supernova remnants -- the remnants of events that took place less than 10^3 years ago, and those more than 10^4 years old. Members of the first class, e.g., Crab Nebula, Tycho's Supernova, and Cas A are visible at energies above 2keV while members of the second class have been seen only below 1keV. The Cygnus Loop belongs to the second class and a recent report by Palmieri et al(10) adds Vela X and Puppis A to this class. The x-ray emission mechanism is known for only one member of the first class, the Crab Nebula and it is synchrotron radiation. Our results suggest that another mechanism, thermal radiation from a hot plasma, is responsible for the emission from the second class.

We acknowledge several informative discussions with Dr. W. Tucker of AS&E, and Dr. R. Angel of Columbia University. This work was supported by the National Aeronautics and Space Administration under Contracts NASW-1889 and NGR 33-008-102.

REFERENCES

1. R.J. Grader, R.W. Hill, J.P. Stoering, Ap. J. L45 (1970).
2. R.C. Henry, G. Fritz, J.F. Meekins, H. Friedman, E.T. Byram, Ap. J. 153, L11 (1968).
3. P. Gorenstein, B. Harris, H. Gursky, R. Giacconi, Nuc. Inst. and Meth. (In Press).
4. D.E. Hogg, Nebulae and Interstellar Matter, B.M. Middlehurst and L.H. Aller, Eds., The University of Chicago Press, Chicago (1968), Chap. II, Plate 4, 5.
5. P. Gorenstein, H. Gursky, G. Garmire, Ap. J. 153, 885 (1968).
6. O.A. Ershov, I.A. Brytov, A.P. Lukirskii, Opt. and Spect. 22, 66 (1967) (translated from Russian).
7. R. Minkowski, Rev. Mod. Phys. 30, 1048 (1958).
8. R.L. Brown and R.J. Gould, Phys. Rev. D 2252 (1970).
9. C.A. Heiles, Ap. J. 140, 470 (1964) and I.S. Shklovsky Supernovae John Wiley, New York (1968).
10. T.M. Palmieri, G. Burginyon, R.J. Grader, R.W. Hill, F.D. Seward, J.P. Stoering UCRL-72614 (1970).

Figure 1. Solid lines are the response of four independent proportional counter elements in focal plane during $1/4^{\circ}$/second scan across Cygnus Loop. Dotted lines represent response of instrument to point source at distance of 80 meters.

Figure 2. Total x-ray data from Cygnus Loop superimposed upon photograph of filaments taken in red light with 48-inch schmidt telescope (Mt. Wilson and Palomar Observatories). Field of view of the instrument is broad along direction of dashed lines.

Figure 3. The points are the pulse height distribution of counts from the Cygnus Loop as observed with this instrument. Smooth curves are the computed response of the instrument to expressions (a) and two cases of expression (b), $B = 0$, and B finite. The line of sight density of interstellar hydrogen is included in the trial functions as a free parameter. Interstellar attenuation accounts for part of the turnover at low energies; the rest is instrumental.

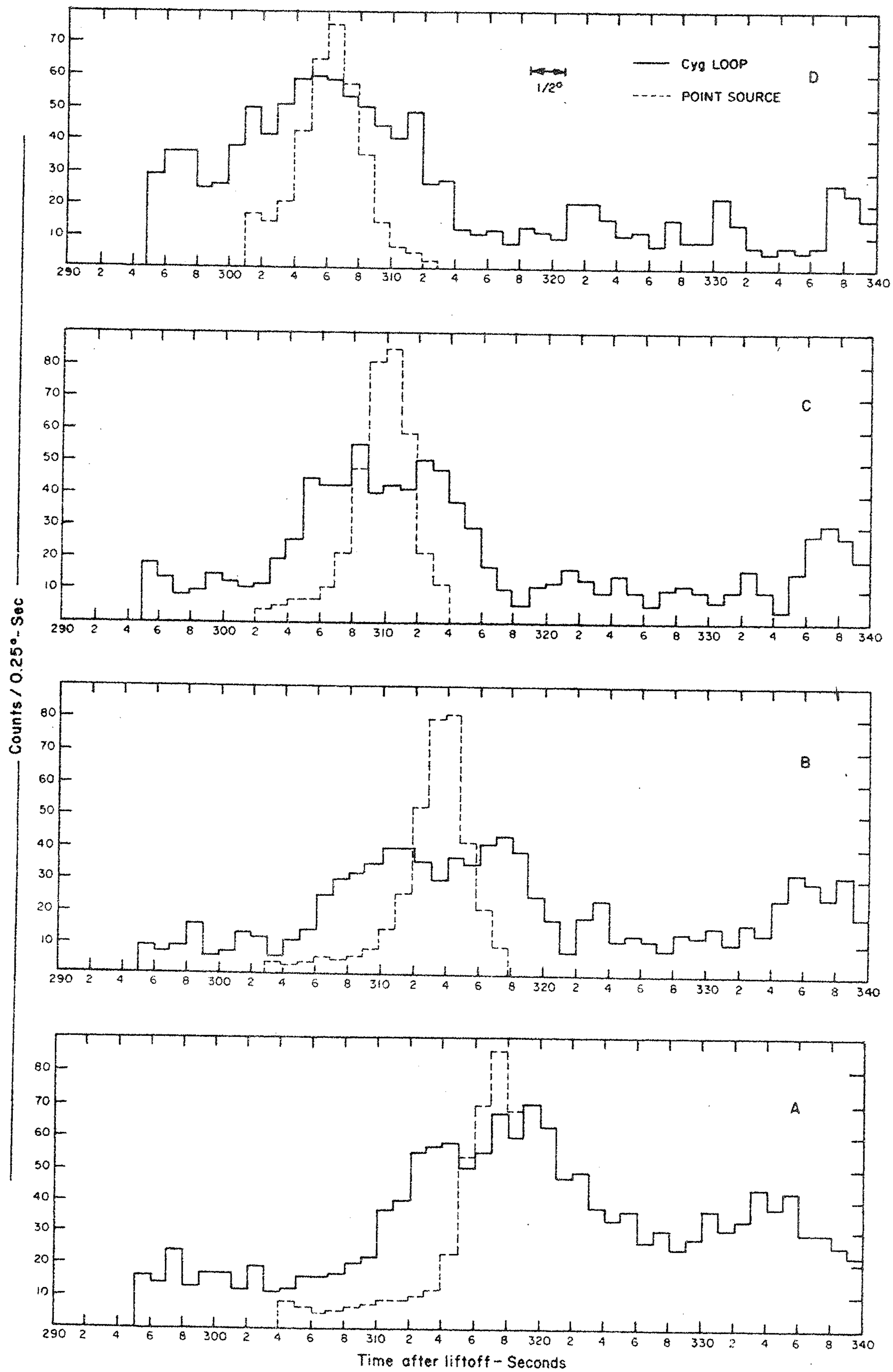
Cyg LOOP
POINT SOURCE
1/2°
D
C
B
A
Counts / 0.25°- Sec
Time after liftoff - Seconds

FIG. 1

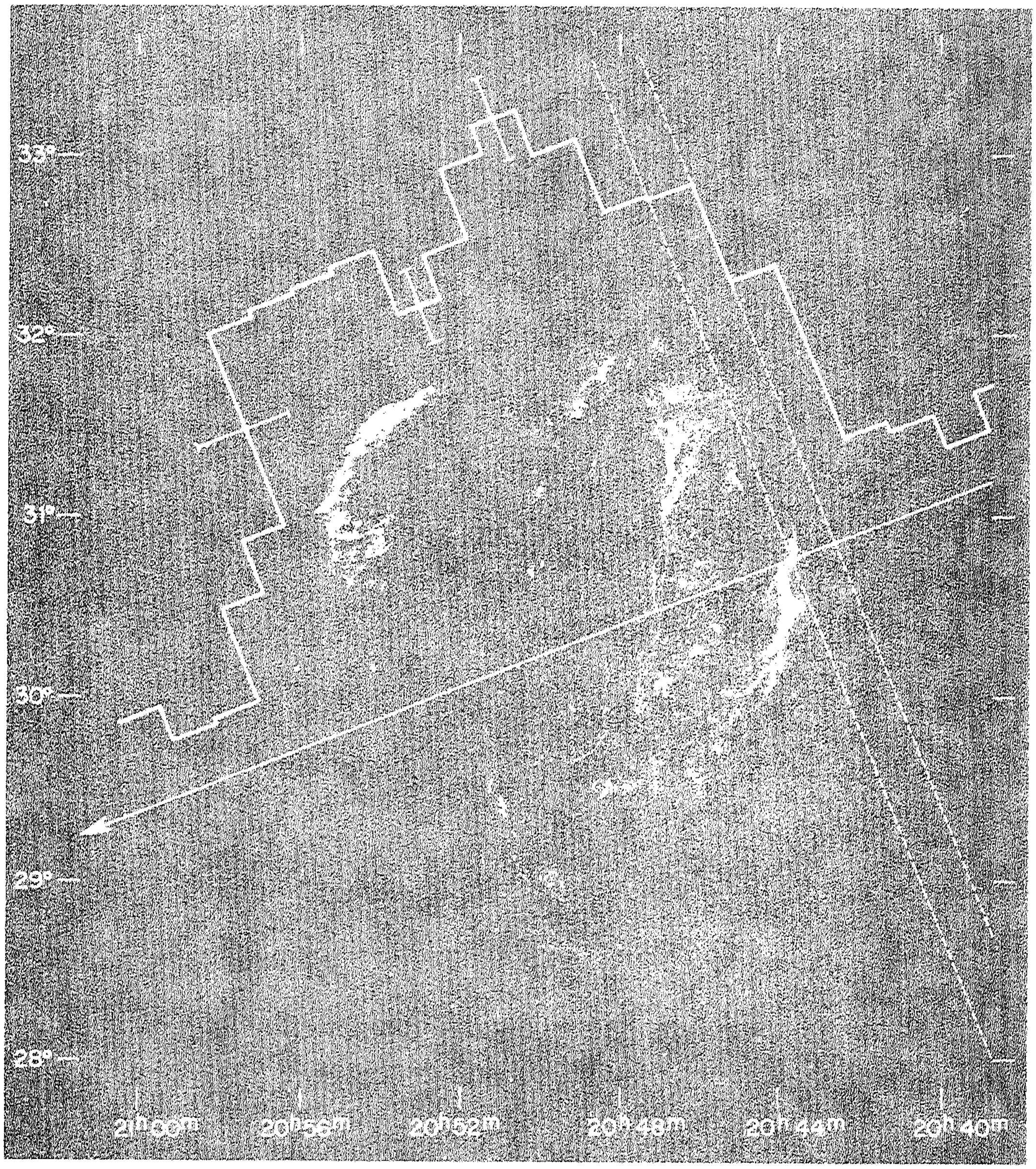

FIG. 2

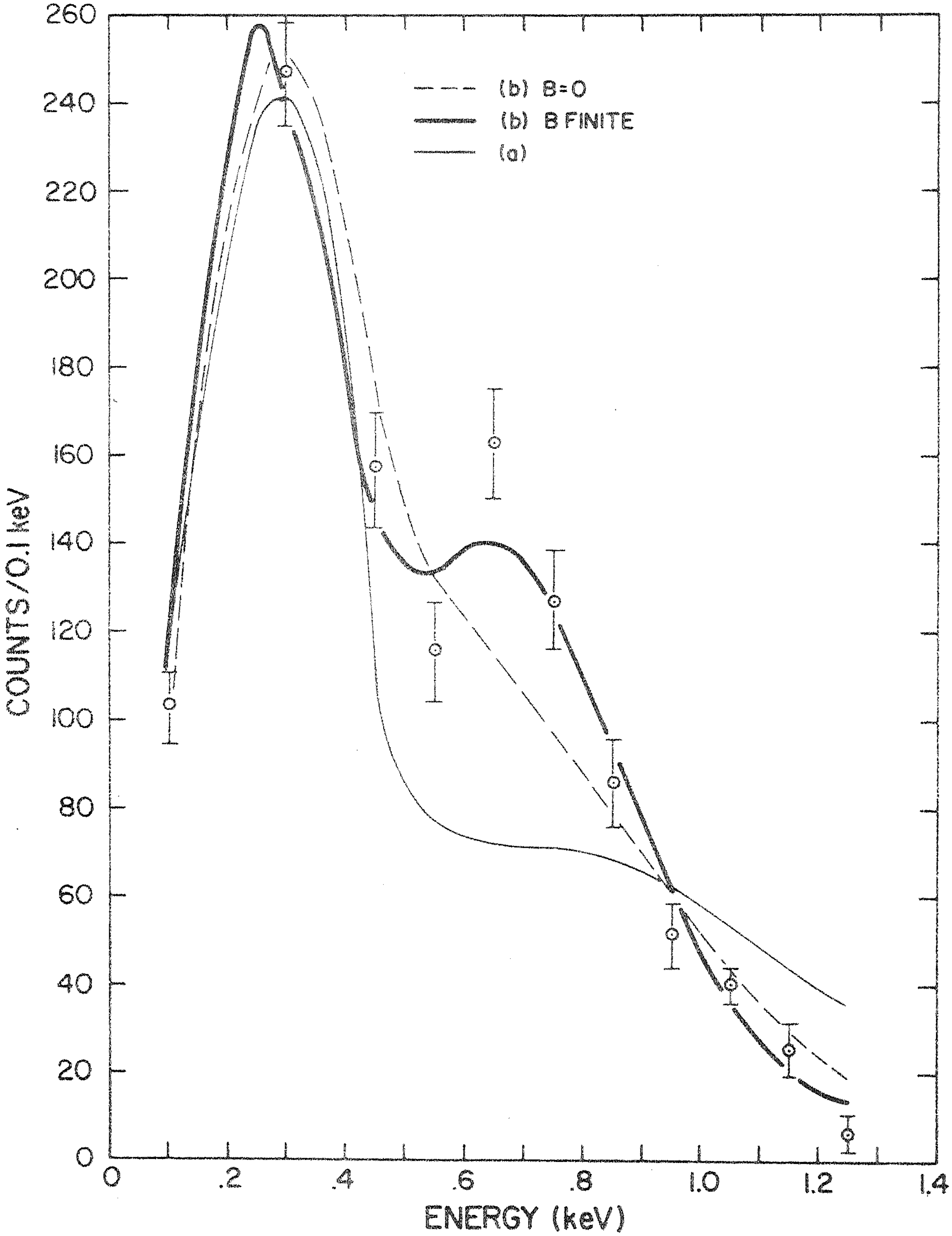

(b) B=0
(b) B FINITE
(a)
COUNTS/0.1 keV
ENERGY (keV)
260
240
220
200
180
160
140
120
100
80
60
40
20
0
0
.2
.4
.6
.8
1.0
1.2
1.4

FIG. 3